Proceedings of the 7th International Conference on Gas Hydrates (ICGH 2011),
Edinburgh, Scotland, United Kingdom, July 17-21, 2011.

GEOMECHANICAL CONSTITUTIVE MODELLING OF GAS-HYDRATE-BEARING SEDIMENTS

Nabil Sultan*
Ifremer, GM/LES
Plouzané, 29280
FRANCE

Sébastien Garziglia
Ifremer, GM/LES
Plouzané, 29280
FRANCE

ABSTRACT

In this work and in order to consider theoretically the effect of gas hydrates on the mechanical properties of their host sediments, hydrate fraction was introduced as a state variable in the framework of a Critical State model. For the proposed model, the process of de-structuration and softening of natural clay was considered as a proxy for the gas-hydrate-bearing-sediments behaviour. The developed constitutive model seemed to reproduce the main key behaviours of gas-hydrate-bearing sands observed by Masui and co-authors: i) the elastic properties (Young Modulus, shear modulus) and the strength of the sediment-hydrate medium increase with the hydrate fraction ii) the mechanical softening of the gas-hydrate bearing sediment is amplified with the hydrate fraction and iii) the dilation angle increases with the hydrate fraction.

Keywords: Constitutive modelling, elasto-plasticity, gas hydrates, sediments, softening.

NOMENCLATURE

a : First fitting parameter for Δv_c [-]

b : Second fitting parameter for Δv_c [-]

$d\varepsilon_v^p$: Volumetric plastic strain increment [-]

$d\varepsilon_s^p$: Plastic shear strain increment [-]

e : Void ratio [-]

E_0, E_η : Young's modulus for, respectively, water saturated and hydrate saturated sediments [kPa]

G_η : Shear modulus for hydrate saturated sediments [kPa]

K_0, K_η : Coefficient of earth pressure at rest for, respectively, water saturated and hydrate saturated sediments [-]

M : Critical state parameter [-]

M_c : Flow rule parameter at which the plastic strains ratio is equal to 0 [-]

p' : Mean effective stress [kPa]

p'_0 : Maximum mean effective stress supported by the sediment [kPa]

p'_c, p'_{c0} : Effective preconsolidation pressure for, respectively, water saturated and hydrate saturated sediments [kPa]

q: Deviatoric stress [kPa]

q_0 : Maximum deviatoric stress supported by the sediment [kPa]

S_h : Degree of hydrate saturation

v : Specific volume

α: First flow rule parameter [-]

β : Slope of the change of the compressibility with the hydrate fraction [-]

* Corresponding author: Phone: +33 2 98224259 Fax +33 2 98224559 E-mail: nabil.sultan@ifremer.fr

Δv_c : Volumetric volume changes generated by hydrate collapse [-]

ε_v : Volumetric strain [-]

ε_s : Shear strain [-]

κ: Cam-Clay elastic compressibility coefficient in e:ln$p$' space [-]

λ_0, λ_1, λ_η : Cam-Clay plastic compressibility coefficient in e:ln$p$' space for, respectively, water saturated sediment, pure hydrate and hydrate saturated sediments

η: Hydrate fraction

μ: Second flow rule parameter [-]

v, v_η : Poisson's ratio for, respectively, water saturated and hydrate saturated sediments [-]

INTRODUCTION

Concerns over gas hydrates in environmental and energy resources issues have found increasing echoes in geomechanics. The practical importance and fundamental interest of analysing submarine slope stability have indeed instigated the development of theoretical models to investigate the response of gas-hydrate-bearing sediments (GHBS) to thermal and/or mechanical solicitations (see [1, 2] and reference therein). As essential inputs into accurate numerical simulations, the mechanical behaviour of GHBS has been extensively studied in laboratory during the last decade. Detailed reviews of laboratory results [3, 4 and 5] point out that upon shearing, the secant stiffness, dilatancy angle, shear strength and brittleness/sensitivity of GHBS tend to increase with hydrate saturation S_h. Such general trends are exhibited for S_h above 25-30 %, when the effective stress progressively looses relevance due to hydrate acting as a bonding agent and/or becoming part of the load-bearing framework [4]. The results of tests conducted on gas hydrates bearing sands revealed that the complex nature of hydrate sediment interaction relies to a significant extent on hydrate growth habits in pore spaces [4, 6]. This may be summarised by noting that hydrate forming in the pore space (pore filling) do not contribute to the stiffness and strength of their host sediment until the creation of weak bonds when S_h rises above 25%. At the other end of the spectrum, hydrates formed at particle contacts tend to contribute to stiffness and strength increases by strongly bonding particles together (cementation) even at low hydrate saturation. Aside from hydrate saturation and growth habits, the behaviour of GHBS has been shown to depend on the strain rate, temperature, consolidation stress, grain size, density, and cage occupancy [7, 8, 9 and 10]. By conducting a series of drained triaxial tests on synthetic methane hydrate-bearing sand specimens with S_h > 35%, Miyasaki et al. [11] emphasised strain rate dependency of the stiffness and peak strength. The fact that a comparatively slight strain rate dependency has been observed for the residual strength suggests that the increase in strain rate tends to promote strain softening.

Kimoto and co-authors recently developed one of the most advanced constitutive models to capture the mechanical behaviour of GHBS. The Kimoto et al. elasto-viscoplastic model [13, 14] is theoretically able to account for the key features of the behaviour of GHBS cited above. In this model, the effect of hydrate saturation is introduced by means of shrinkage or expansion of the overconsolidation boundary surface and the static yield surface. A hardening-softening rule accounting for the effect of suction, hydrate saturation, and structural degradation with increasing viscoplastic strain adds to the sophistication of the Kimoto et al's model. However, to the best of our knowledge, the performance of this model for the simulation of data obtained from laboratory testing on GHBS has not yet been emphasised.

Due, on one hand, to the number of mechanisms considered in the Kimoto et al's model and, on the other hand, to the important number of input model parameters, we propose in the present work a new simple constitutive model where the hydrate fraction is introduced as a state variable in the framework of a Critical State model. With some analogies with the approach proposed by [13, 14], the proposed elasto-plastic constitutive model considers the effect of gas hydrates through the hydrate fraction which controls the size and orientation of the yield surface. This aims at evaluating the application of the critical state soil mechanics to developing an understanding of the response of GHBS.

MECHANICAL MODEL FOR GHBS SEDIMENTS

Model formulation for isotropic stress states

The effect of gas hydrates on their host sediment is considered similar to the de-structuration and softening of natural clay where i) the hydrate formation impedes the normal consolidation of the

sediment along the normal consolidation line (*NCL*) due to the rigidity and stiffness of the cementing agent and ii) the dissolution/dissociation and/or mechanical loading may lead to the compaction (collapse) of the sediment in order to reach the related compressibility line which is characterized by a plastic compressibility coefficient λ_η [15] (Figure 1).

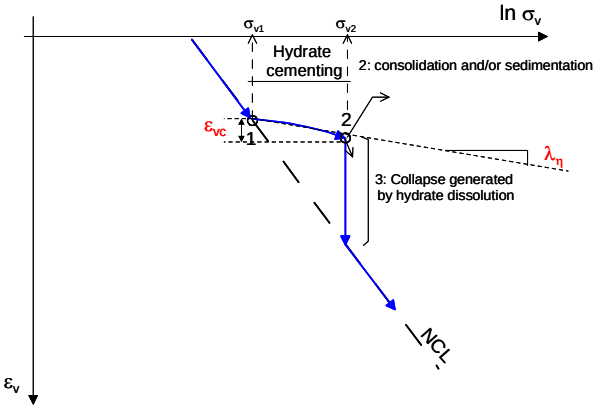

Figure 1: Schematic description of the development of cementing structure in GHBS which impedes the normal consolidation of the sediment along the *NCL*.

The determination of the GHBS compressibility is based on the following hypothesis [16]: the plastic compressibility of the gas-hydrate bearing sediments decreases from the slope of the *NCL* for purely water saturated soil and tends asymptotically to the pure hydrate compressibility which was identified to be equal to 0.00147 [17]. The change of λ_η with η is considered through the following equation:

$$\lambda_\eta = \lambda_0\left[1-\left(1-\frac{\lambda_1}{\lambda_0}\right)\left(1-\exp\left(-\beta.\eta\right)\right)\right] \qquad [1]$$

where λ_0 is the plastic compressibility coefficient of water saturated sediment, β defines the slope of the change of the compressibility with the hydrate fraction (Figure 2), λ_1 is the plastic compressibility coefficient of the hydrate phase.

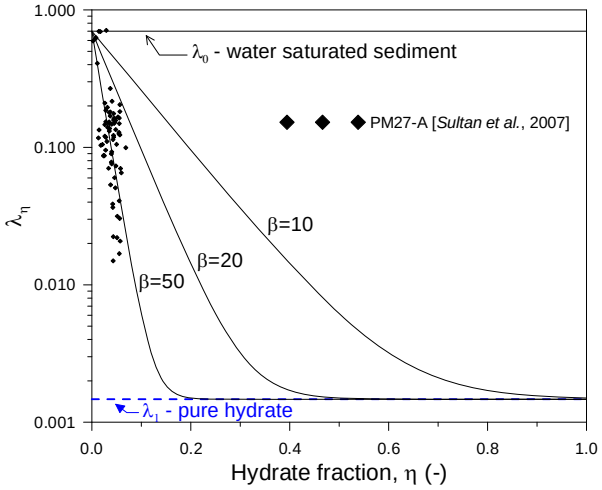

Figure 2: λ_η as a function of the hydrate fraction for three different values of β. Dots correspond to λ_η obtained from in situ piezocone data [18].

The isotropic formulation is carried out in the specific volume ($v=1+e$)/mean effective stress (p') space. This formulation is similar to the one developed by [19] for the isotropic formulation for unsaturated soil. From this isotropic formulation, the effective preconsolidation pressure p'_c is found equal to:

$$p'_c = p'_{c0}.\exp\left[\frac{\left(\lambda_0-\lambda_\eta\right).\ln\left(\frac{p'_{c0}}{p'_c}\right)+\Delta v_c}{\lambda_0-\lambda_\eta}\right] \qquad [2]$$

Where Δv_c corresponds to the volumetric volume changes generated by hydrate collapse and it depends on η through two fitting parameters a and b.

Model formulation for triaxial stress states

The shear modulus G_η is considered as a function of η through the Young's modulus and is given by the following equation:

$$G_\eta = \frac{\left(E_0+\eta.E_\eta\right)}{2\left(1+\nu_\eta\right)} \qquad [3]$$

The assumption of a linear relationship between the Young's modulus and the hydrate saturation is

supported by experimental results reported by [3] and [4].
The coefficient of earth pressure at rest is also taken as a function of η through the parameter β and is given by:

$$K_\eta = (K_0 - 1).\exp(-\beta.\eta) + 1 \quad [4]$$

The Poisson ratio ν_η is calculated using the following equation:

$$\nu_\eta = \frac{K_\eta}{1 + K_\eta} \quad [5]$$

The deviatoric water-saturated model adopted as a limit condition is a version of the Banerjee et al's model [20] which was developed in order to take into account the initial anisotropy of natural clay and the enhanced anisotropy generated by different stress paths.

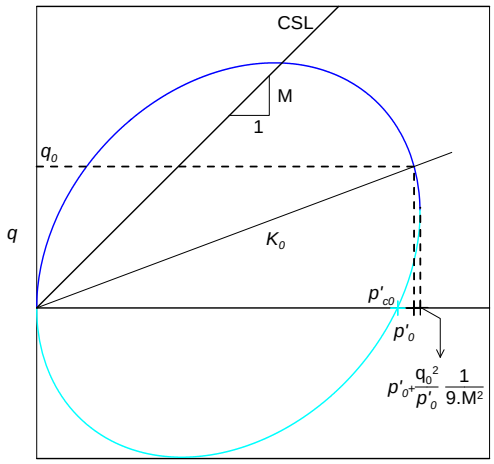

Figure 3: Yield curve in the deviatoric stress-mean effective stress diagram [20].

Under axisymetric loading conditions (radial stresses are equal – condition of triaxial test), the yield curve is given by the following equation [20]:

$$q = \frac{2}{3} p' \frac{q_0}{p'_0} \pm \sqrt{M^2 \left(p' p'_0 - p'^2\right) + \frac{1}{9} \frac{p'}{p'_0} q_0^2} \quad [6]$$

where q and p' are respectively the deviatoric and mean effective stress, M is the slope of the critical state line, and q_0 and p'_0 are the projection of the additional stress tensor in the q-p' diagram (Figure 3) and correspond for a saturated soil to the maximum loading supported by the sediment. q_0 is related to p'_0 through the following equation:

$$q_0 = -3p'_0 \frac{K_\eta - 1}{2K_\eta + 1} \quad [7]$$

The use of inclined yield curves to account for induced anisotropy is of great interest considering that gas-hydrate occurrence may affect the initial anisotropy of natural, water-saturated sediments. This initial anisotropy is indeed likely to become secondary when hydrates nucleate and grow isotropically in the host medium (Figure 4).

In addition to the two hardening laws proposed by [20], an expansion of the yield curve is also generated by the hydrate formation which leads, as discussed earlier, to an increase of the preconsolidation pressure p'_c and therefore to an increase of p'_0 (Figure 3 and equation 2).

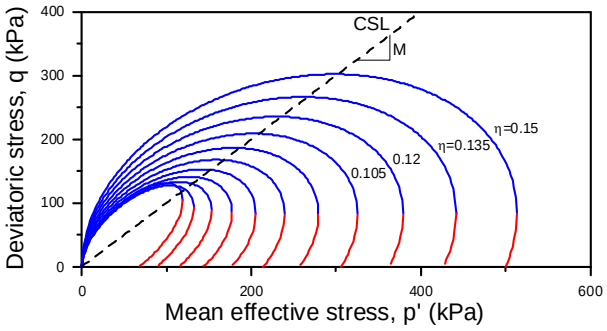

Figure 4: Hardening of the Banerjee yield curve. The increase of the hydrate fraction reduces initial anisotropy of the water-saturated sediment.

In most constitutive models for saturated soils, the plastic potential only depends on the stress inclination q/p' [21, 22 and 23]. For this reason, the determination of the flow rule can be done by plotting the direction of plastic strains ratio $\frac{d\varepsilon_v^p}{d\varepsilon_s^p}$ as a function of stress ratio $\frac{q}{p'}$. In this work we used the expression proposed by Lagioia et al. [24] which depends on three parameters: μ, α, Mc.

PARAMETERS OF THE MODEL AND THEIR DETERMINATION

In total, twelve parameters (κ, λ, M, E_0, E_η, μ, α, Mc, a, b, β) are introduced in the proposed model. They can be determined as follows:

- a) κ, λ, M are common Cam-clay parameters that can be easily determined;

-b) E_0, E_η from at least two triaxial shearing tests at two different hydrate concentrations.

-c) μ, α, Mc are 3 parameters for the flow rule and are calculated by using the $(d\varepsilon_v^p / d\varepsilon_s^p) - (q/p')$ curves.

(d) a, b, β govern the shape of the yield surface in the q-p'-η space and can be derived from at least two isotropic tests at two different hydrate concentrations.

MODEL PERFORMANCE

The constitutive model here proposed to simulate GHBS behaviour was coded in FORTRAN. The aim of this paragraph is to show the capability of the model for some selected stress paths under drained conditions. A single set of model parameters is used to represent the reference sediment:

- Cam-Clay parameters:, κ = 0.05, λ=0.5, M=1.35
- Shear modulus, G_η: E_0=112880 kPa, E_η=680410 kPa,
- Flow rule: μ = 1.2, α = 0.001, Mc = 1.45
- Compressibility and collapse: a=1.8, b=4.050 and β=10.
- Banerjee yield curve: K_0 = 1.0

Figure 5 shows the compressibility curves obtained from simulations of drained isotropic loading at 4 different initial hydrate fractions. The initial hydrate fractions are between 0% and 25%. Figure 5 shows that the effective preconsolidation pressure and therefore the size of the yield curve and the collapse volumetric strain both increase with η while the compressibility decreases with the increase of η.

Figure 6 shows 4 stress paths in deviatoric-mean effective stress diagram of GHBS under drained isotropic loading at 4 different initial hydrate fractions. The expansion of the yield curve due to the hydrate fraction is associated with a decrease of the initial anisotropy of the hydrate-sediment system.

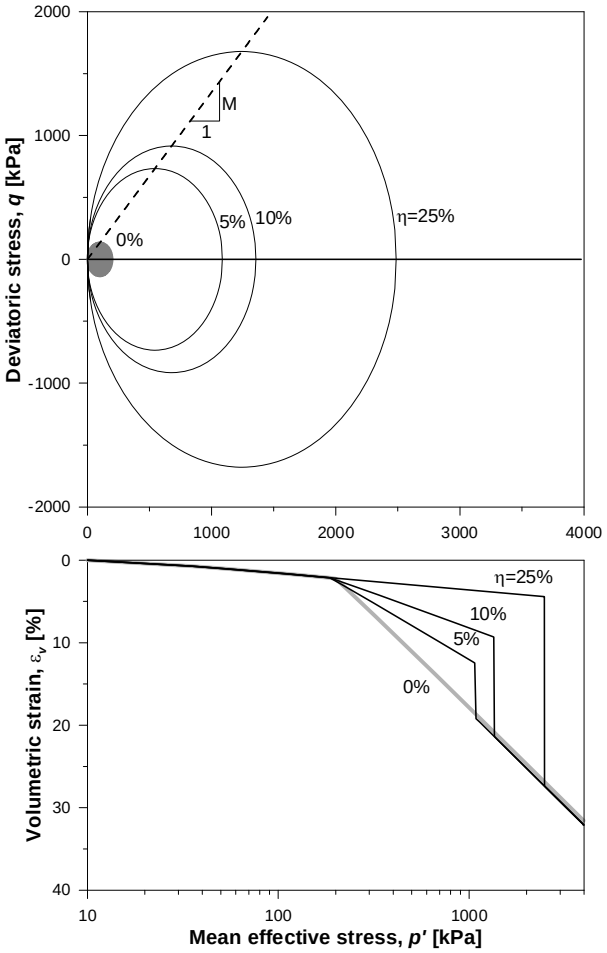

Figure 5: Mechanical collapse of GHBS under drained isotropic loading at different initial hydrate fractions.

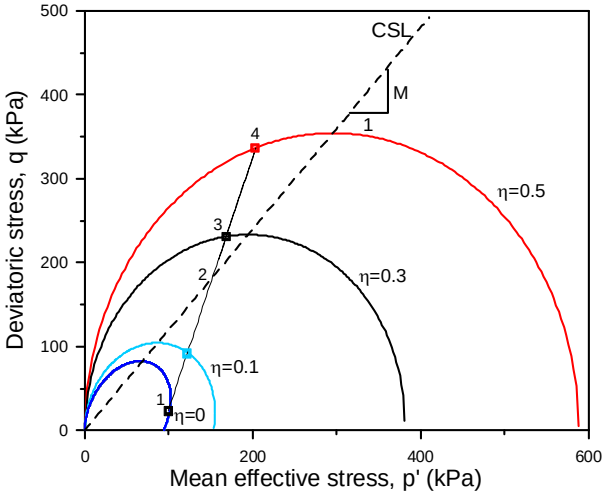

Figure 6: Stress path in deviatoric-mean effective stress diagram of GHBS under drained isotropic loading at 4 different initial hydrate fractions.

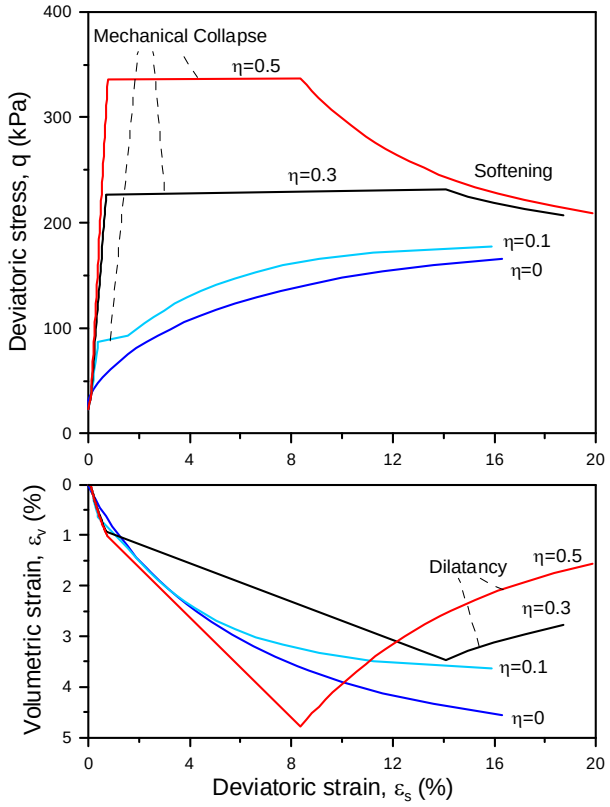

Figure 7: Deviatoric behaviour of GHBS under drained loading at different initial hydrate fractions. a) Deviatoric stress and strain relationship b) volumetric strain and deviatoric strain relationship.

The deviatoric stress and strain relationship and the volumetric strain and deviatoric strain relationship are presented in Figure 7. The deviatoric behaviour depends strongly on the initial hydrate fraction going from normal hardening of the water saturated sample (η = 0) to a collapse of the material followed by hardening (η = 10%) and softening of the hydrate-sediment system (η = 30% and 50%). The increase of the stiffness of the hydrate-sediment system can be also observed in Figure 7. The volumetric strain and deviatoric strain relationships presented in Figure **7** show how the dilatancy angle increases with η.

MODELLING SOME EXISTING DATA

Tests on natural methane hydrate bearing sediment samples [9]

In the following, the proposed constitutive model is used to simulate triaxial drained tests published by [9]. Those tests were carried out on natural sandy methane hydrate samples retrieved from the Nankai Trough with hydrate saturations between 7.7 and 37.6%. Samples were consolidated isotropically at cell pressure of 10 MPa and back pressure of 9 MPa (the initial effective confining pressure is 1 MPa). Samples were then sheared in compression at an axial strain rate of 0.1 %/min (more details in [3]). Two of the tests (S_h of 7.7% and 37.6%) presented in Figure 8 were used to define the set of model parameters:

- Cam-Clay parameters:, κ = 0.03, λ=0.05, M=1.35
- Shear modulus, G_η: E_0=112880 kPa, E_η=680410 kPa,
- Flow rule: μ = 0.8, α = 0.001, Mc = 1.45
- Compressibility and collapse: a=0.1115, b=8.050 and β=15.
- Banerjee yield curve: K_0 = 0.5

Figure 8 shows a comparison of the experimental results reported by [9] and model predictions. Yield curves are presented in a q-p' diagram (Figure 8-a), stress-strain curves in q-ε_s diagram are presented in Figure 8-b, strains in ε_v-ε_s diagram are presented in Figure 8-c and strain-stress curves in p'-ε_v diagram are shown in Figure 8-d. Results in Figure 8 show an overall reasonable agreement between experimental and predicted curves. The predicted results are able to reproduce qualitatively the following key features of behaviour of gas hydrates bearing sands: increase of the shear modulus, peak shear strengths, dilatancy angles and strain softening rates with hydrate saturation. Moreover, the proposed constitutive model is also able to reproduce quantitatively strain and stress experimental curves for S_h of 7.7%, 9.38% and 37.6%. For S_h of 22.5%, modelling results failed to reproduce quantitatively the experimental data. Also, the post peak stress-strain behaviour obtained using the proposed model is not able to reproduce the smooth strain softening observed for natural gas hydrate bearing sediments. Indeed, the model predicts a two post-peak phases with a collapse followed by a strain softening (Figure 8-b).

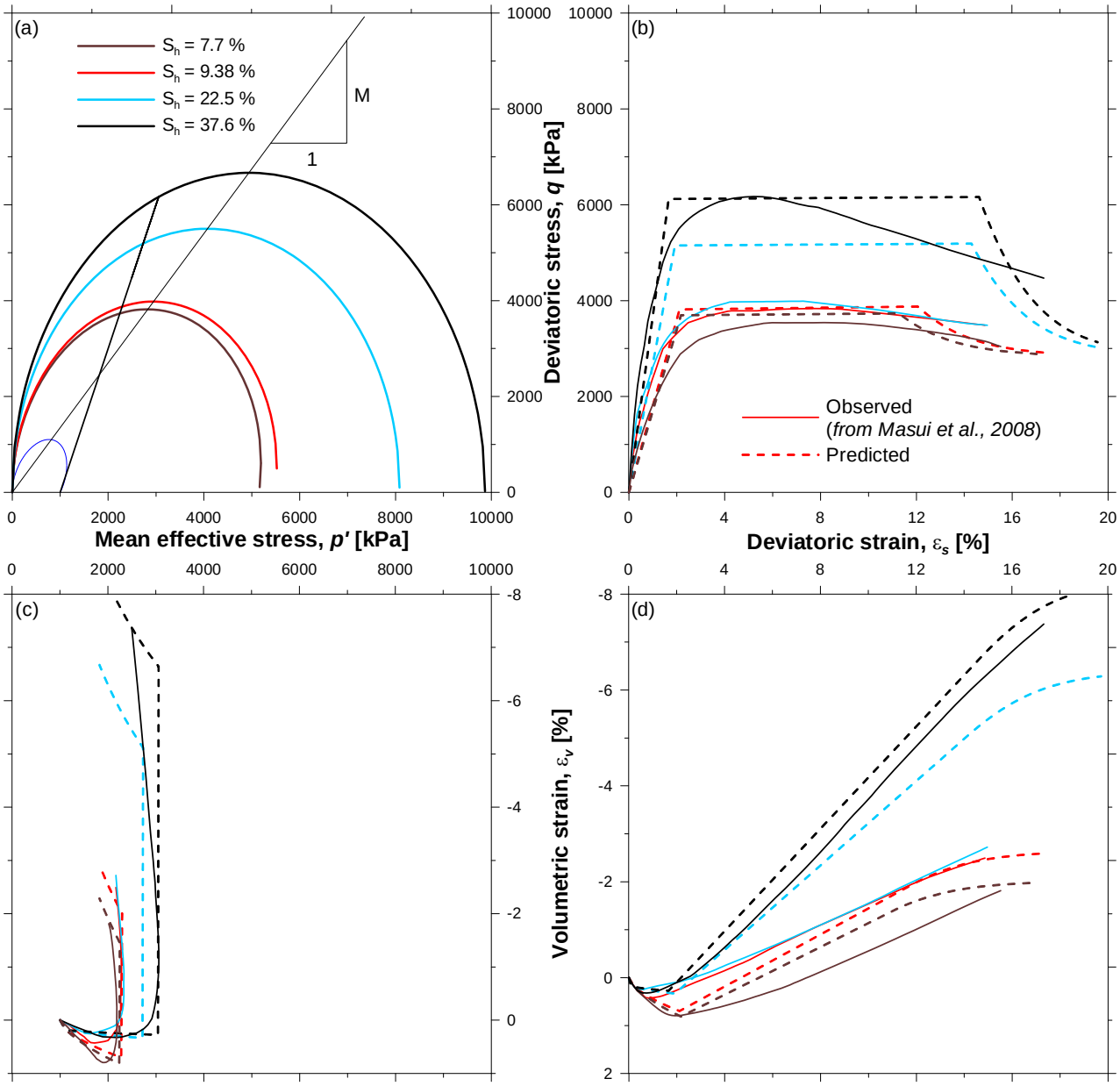

Figure 8: Synthetic presentation of drained triaxial tests carried out on Nankai Trough natural methane hydrate bearing sediment samples [9] and predicted results obtained using the proposed constitutive model. a) yield curves in p'-q diagram, b) stress-strain curves in q-ε_s diagram, c) strains in ε_v-ε_s diagram and d) strain-stress curves in p'-ε_v diagram. Continuous lines correspond to experimental data and dashed lines to predicted results.

Tests on synthetic hydrate sample (from [25])

Masui et al. [25] carried out tests on synthetic methane hydrate specimens with different hydrate growth habits in the pores of Toyoura sand. Samples with weak and strong contact bonds were created, depending on the method of hydrate formation [3].

Four sand samples were submitted to a confining effective stress of 1 MPa (9 MPa of confining pressure and a back pressure of 8 MPa). They were then sheared at a constant rate of 0.1%/min in drained conditions (more details in [3]). The degree of hydrate saturation ranged between 0% and 55.1%. Two of the experimental tests presented in Figure 9 (S_h of 0% and 55.1%) were used to define the set of model parameters:

- Cam-Clay parameters:, κ = 0.03, λ=0.05, M=1.55

- Shear modulus, G_η: E_0=170000 kPa, E_η=680410 kPa,
- Flow rule: μ = 1.2, α = 0.001, Mc = 1.65
- Compressibility and collapse: a=0.13, b=3.65 and β=15.
- Banerjee yield curve: K_0 = 1

The use of K_0 equal 1 expresses the initial isotropic state of the synthetic tested sands.

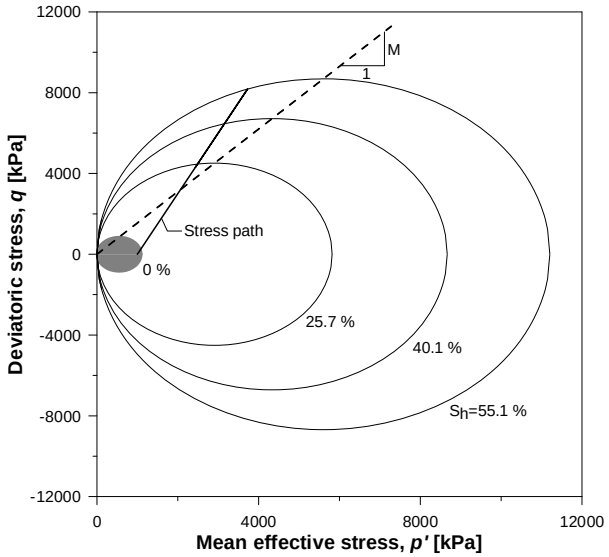

Figure 9: Strong bond - Hardening of the yield curve: from an initial water saturated sands to sands with a hydrate saturation of 55.1%.

Figure 9 shows, for the strong-bond hydrate-sediment samples, the predicted hardening of the yield curve as a function of the hydrate saturation. The effective preconsolidation pressure increases from 1 MPa for S_h=0% to around 10.2 MPa for S_h=55.1%.

Experimental and predicted stress-strain curves are presented in Figure 10 in q-ε_s diagram. As for the natural methane hydrate bearing sediment samples, the constitutive model is able to reproduce the increase of the stiffness, peak shear strengths, dilatancy angles and strain softening rates with hydrate saturation.

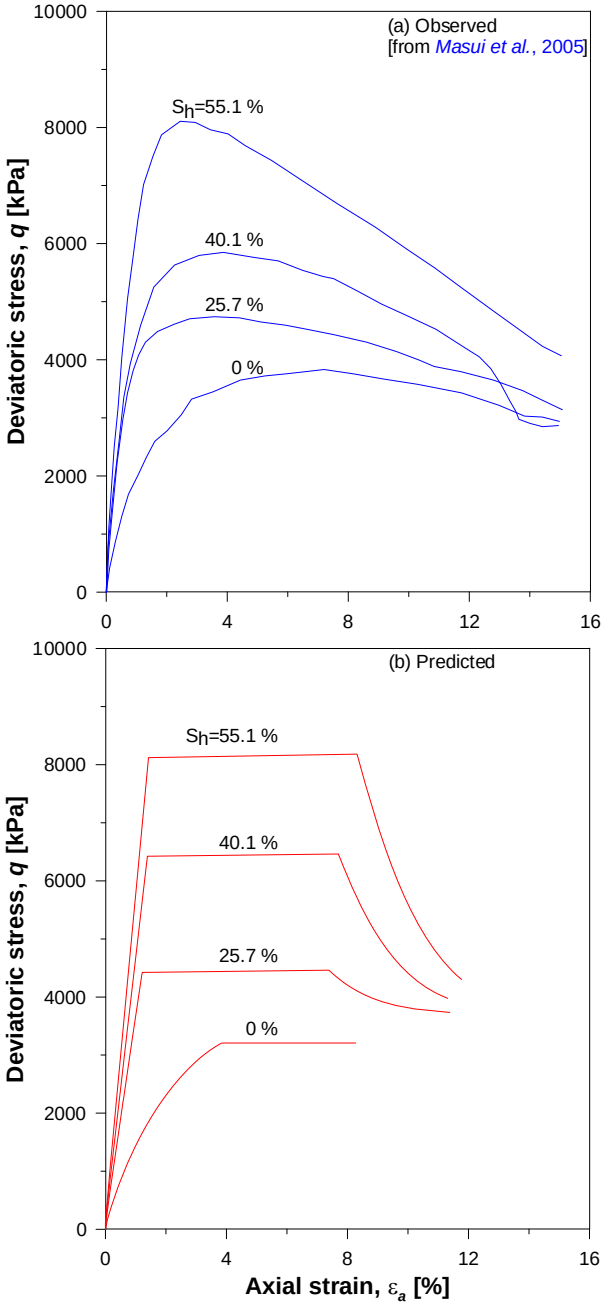

Figure 10: Strong bond - Deviatoric behaviour of GHBS under drained loading at different initial hydrate fractions: a) observed [25] versus b) predicted curves.

It can also be seen from Figure 10 that the model quantitatively reproduces the experimental data for the 4 degrees of hydrate saturation: 0%, 25.7%, 40.1% and 55.1%. However, and as in the case of the previous calculation, the model does not fit quite as well the smooth post-peak strength reduction characterising the experimental results.

In the Masui et al. [25] paper, four weak-bond hydrate-sediment samples were also submitted to a confining effective stress of 1 MPa (9 MPa of confining pressure and a back pressure of 8 MPa). Subsequently, the four samples were sheared at a constant rate of 0.1%/min in drained conditions (more details in [3]). The degree of hydrate saturation ranged between 0% and 67.8%.

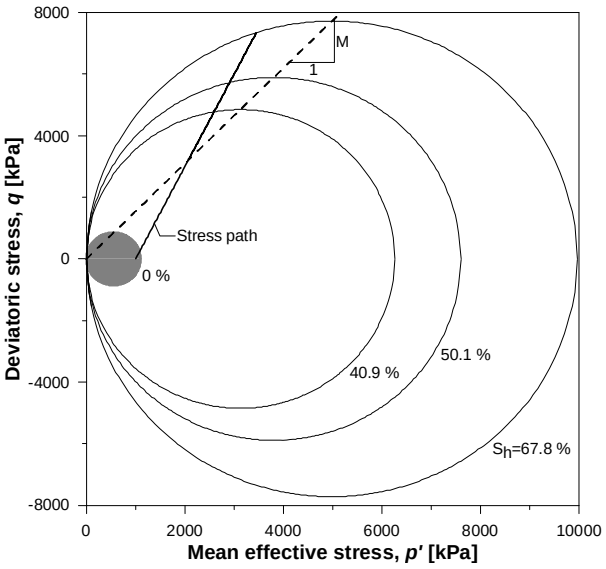

Figure 11: Weak bond - Hardening of the yield curve: from an initial water saturated sands to sands with a hydrate saturation of 67.8%.

Two of the experimental tests presented in Figure 9 (S_h of 0% and 67.8%) were used to define the set of model parameters:

- Cam-Clay parameters:, $\kappa = 0.03$, $\lambda=0.05$, $M=1.55$
- Shear modulus, G_η: $E_0=170000$ kPa, $E_\eta=680410$ kPa,
- Flow rule: $\mu = 1.2$, $\alpha = 0.001$, $Mc = 1.65$
- Compressibility and collapse: $a=0.13$, $b=2.55$ and $\beta=15$.
- Banerjee yield curve: $K_0 = 1$

Figure 11 shows for the weak-bond hydrate-sediment samples the predicted expansion of the yield curve as a function of the hydrate saturation. The effective preconsolidation pressure increases from 1 MPa for S_h=0% to around 9.9 MPa for S_h=67.8%.

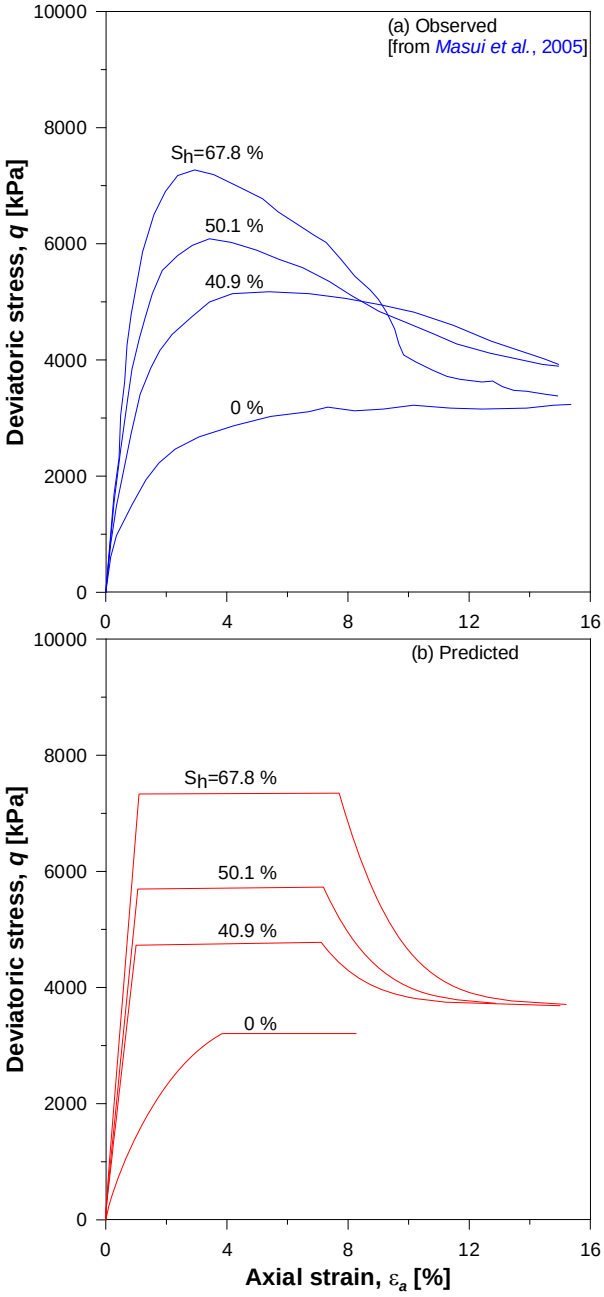

Figure 12: Weak bond - Deviatoric behaviour of GHBS under drained loading at different initial hydrate fractions: a) observed [25] versus b) predicted curves.

Experimental and predicted stress-strain curves are presented in Figure 12 in q-ε_s diagram. It can be seen from Figure 12 that the model predictions are both qualitatively and quantitatively consistent with the experimental data for the 4 degrees of hydrate saturation: 0%, 40.9%, 50.1% and 67.8%. The weak point of those predictions is the simulated post peak stress-strain behaviour which

is not able to reproduce the observed smooth strain softening behaviour.

UNCERTAINTIES AND WAY FORWARD

The proposed constitutive model was developed by considering the following two main assumptions:

- Hydrate formation impedes the normal consolidation of the sediment along the normal consolidation line (*NCL*). Subsequent mechanical loading leads to the compaction (collapse) of the sediment in order to reach the NCL.
- The plastic compressibility of the gas-hydrate bearing sediments decreases from the slope of the *NCL* for purely water saturated soil and tends asymptotically to the pure hydrate compressibility;

Although in situ piezocone data acquired from the deep water Niger Delta [18] show, indirectly and empirically, a link between the plastic compressibility and the hydrate concentration, it is today essential to validate the proposed relationship through laboratory tests. Furthermore, the evolution of the preconsolidation pressure as a function of the degree of hydrate saturation, the collapse process, and finally the uniqueness of the *NCL* after the collapse process would need experimental validations.

The validation of the proposed constitutive model was done by simulating experimental data carried out on natural and artificial sand samples. The characterization of the mechanical properties of gas-hydrate-bearing sand is essential for gas production from gas hydrates sandy/silty reservoirs. However, several geomechanical applications (submarine slope instabilities, ground deformations near and below foundations and pipelines,…) need an accurate mechanical characterization of gas-hydrate-bearing clay. One of the most important features that may differ between gas-hydrate-bearing sands and clays is the volumetric strain during drained shearing. While it seems clear that dilatancy occurs and increases with the hydrate saturation for sands, to date uncertainties remains as to whether the same applies for gas-hydrate-bearing clays. Actually, in situ piezocone testing in hydrate-clayey sediments [18] showed an important increase of the pore water pressure suggesting a shear-enhanced compaction rather than dilatancy of the materials as observed on laboratory tests conducted by [26] on kaolinite samples containing tetrahydrofuran hydrate.

The proposed constitutive model was also able to reproduce one of the main features of available experimental data showing that an increase in gas hydrates content tend to increase the value of the peak shear strength without affecting its residual value [9 and 25]. By promoting strain softening, the presence of gas hydrates could have detrimental consequences if field operations and installations causes significant mechanical loading. Indeed, strain softening may completely erase the strengthening effect of gas hydrates on their host sediments.

REFERENCES

[1] Grozic, J.L.H. *Interplay between gas hydrates and submarine slope failure*. In : Mosher et al. editors. Submarine Mass Movements and Their Consequences, Advances in Natural and Technological Hazards Research (28), 2010. p. 11-30.

[2] Moridis, G.J., Collett, T.S., Pooladi-Darvish, M., Hancock, S., Santamarina, C., Boswell, R. Kneafsey, T., Rutqvist, J., Kowalsky, M.B., Reagan, M.T., Sloan, E.D., Sum, A.K., Koh, C.A. *Challenges, uncertainties, and issues facing gas production from gas-hydrate deposits*. SPE Reservoir Evaluation and Engineering 2011; 14(1):76-112.

[3] Soga, K., Lee, S.L., Ng, M.Y.A., Klar, A. *Characterisation and engineering properties of methane hydrate soils*. In : Tan, T.S., et al., editors. Characterization and Engineering Properties of Natural Soils. London: Taylor and Francis, 2006. 4. p.2591-2642.

[4] Waite, W.F., Santamarina, J.C., Cortes, D.D., Dugan, B., Espinoza, D.N., Germaine, J., Jang, J., Jung, J.W.T., Kneafsey, T., Shin, H., Soga, K., Winters, W.J., Yun, T.S. *Physical properties of hydrate-bearing sediments*. Reviews of Geophysics 2009; 47, RG4003.

[5] Grozic, J.L.H., Ghiassian, H. *Undrained shear strength of methane hydrate-bearing sand; preliminary laboratory results*. In : Proceedings of the 63rd Canadian Geotechnical Conference, GEO2010, Calgary, 2010.

[6] Clayton, C.R.I., Priest, J.A., Rees, E.V.L. *The effects of hydrate cement on the stiffness of some sands*. Géotechnique 2010; 60(6): 435-445.

[7] Winters, W.J., Pecher, I.A., Waite, W.F., Mason, D.H. *Physical properties and rock physics models of sediment containing natural and*

laboratory-formed methane gas hydrate. American Mineralogist 2004; 89:1221-1227.
[8] Masui, A, Miyazaki, K., Haneda, H., Ogata, Y, Aoki, K. *Mechanical properties of natural gas hydrate bearing sediments retrieved from Eastern Nankai trough*. In: Conference, O.T. (Ed.), Offshore Technology Conference. OTC, Houston, Texas, 2008. p. 19277.
[9] Masui, A., Miyazaki, K., Haneda, H., Ogata, Y., Aoki, K. *Mechanical characteristics of natural and artificial gas hydrate bearing sediments*. In : Proceedings of the 6th International Conference on Gas Hydrates, Vancouver, 2008.
[10] Miyazaki, K., Masui, A., Haneda, H. Ogata, Y., Aoki, K., Yamaguchi, T. *Variable-compliance-type constitutive model for methane hydrate bearing sediment*. In : Proceedings of the 6th International Conference on Gas Hydrates, Vancouver, 2008.
[11] Miyazaki, K., Masui, A., Sakamoto, Y., Tenma, N. *Effect of confining pressure on triaxial compressive properties of artificial methane hydrate bearing sediments*. In : Conference, O.T. (Ed.), Offshore Technology Conference. OTC, Houston, Texas, 2010. p. 20721.
[12] Miyazaki, K., Masui, A., Aoki, K., Sakamoto, Y., Yamaguchi, T., Okubo, S. *Strain-rate dependence of triaxial compressive strength of artificial methane-hydrate-bearing sediment*. International Journal of Offshore and Polar Engineering 2010; 20(4): 256-264.
[13] Kimoto, S., Oka, F., Fushita, T., Fujiwaki, M. *Chemo-thermo-mechanically coupled numerical simulation of the subsurface ground deformations due to methane hydrate dissociation*. Computers and Geotechnics 2007; 34:216-228.
[14] Kimoto, S., Oka, F., Fushita, T. *A chemo–thermo–mechanically coupled analysis of ground deformation induced by gas hydrate dissociation*. International Journal of Mechanical Sciences 2010; 52:365-376.
[15] Sultan, N. *Comment on "Excess pore pressure resulting from methane hydrate dissociation in marine sediments: A theoretical approach" by Wenyue Xu and Leonid N. Germanovich*. Journal of Geophysical Research 2007; 112, B02103.
[16] Sultan, N., Marsset, B., Ker, S., Marsset, T., Voisset, M., Vernant, A.M., Bayon, G., Cauquil, E., Adamy, J., Colliat, J.L., Drapeau, D. *Hydrate dissolution as a potential mechanism for pockmark formation in the Niger Delta*. Journal of geophysical research 2010; 115, B08101.
[17] Durham, W.B., Kirby, S.H., Stern, L.A., Zhang, W. *The strength and rheology of methane clathrate hydrate*. Journal of Geophysical Research 2003; 108(B4), 2182.
[18] Sultan, N., Voisset, M., Marsset, T., Vernant, A.M., Cauquil, E., Colliat, J.L., Curinier, V. *Detection of free gas and gas hydrate based on 3D seismic data and cone penetration testing: An example from the Nigerian Continental Slope*. Marine Geology 2007; 240:235–255.
[19] Alonso, E.E., Gens, A., Josa, A. *A constitutive model for partially saturated soils*. Géotechnique 1990; 40(3):405-430.
[20] Banerjee, P.K., Stipho, A.S., Yousif, N.B. A *Theoretical and experimental investigation of the behaviour of anisotropically consolidated clay*. In : Banerjee, P.K and Butterfield, R., editors. Developments in soil mechanics and foundation engineering, vol. 2. Elsevier Applied Science Publishers, 1986. p. 1-41.
[21] Roscoe, K.H. and Burland, J.B. *On the generalized stress-strain behaviour of "Wet" clay*. In: Heyman, J., and Leckie, F.A., editors. Engineering Plasticity. Cambridge University Press, 1968. p. 535-610.
[22] Wong, P.K.K., Mitchell, R.J. *Yielding and plastic-flow of sensitive cemented clay*. Géotechnique 1975; 25:763-782.
[23] Nova, R., Wood, D.M. A *constitutive model for sand in triaxial compression*. International Journal for Numerical and Analytical Methods in Geomechanics 1979; 3:255-278.
[24] Lagioia, R., Puzrin, A.M., Potts, D.M. *A new versatile expression for yield and plastic potential surfaces*. Computers and Geotechnics 1996; 19(3):171-191.
[25] Masui, A., Haneda, H., Ogata, Y., Aoki, K. *Effects of methane hydrate formation on shear strength of synthetic methane hydrate sediments*. In: Proceedings of the 15th International Offshore and Polar Engineering Conference, Seoul, 2005. p. 364-369.
[26] Yun, T.S., Santamarina, J.C., Ruppel, C. *Mechanical properties of sand, silt, and clay containing tetrahydrofuran hydrate*. Journal of Geophysical Research 2007 ; 112, B04106.